LETTER

doi:10.1038/nature11511

Unexpectedly large mass loss during the thermal pulse cycle of the red giant star R Sculptoris

M. Maercker[1,2], S. Mohamed[3], W. H. T. Vlemmings[4], S. Ramstedt[2], M. A. T. Groenewegen[5], E. Humphreys[1], F. Kerschbaum[6], M. Lindqvist[4], H. Olofsson[4], C. Paladini[6], M. Wittkowski[1], I. de Gregorio-Monsalvo[7] & L.-A. Nyman[7]

The asymptotic-giant-branch star R Sculptoris is surrounded by a detached shell of dust and gas[1,2]. The shell originates from a thermal pulse during which the star underwent a brief period of increased mass loss[3,4]. It has hitherto been impossible to constrain observationally the timescales and mass-loss properties during and after a thermal pulse—parameters that determine the lifetime of the asymptotic giant branch and the amount of elements returned by the star. Here we report observations of CO emission from the circumstellar envelope and shell around R Sculptoris with an angular resolution of 1.3″. What was previously thought to be only a thin, spherical shell with a clumpy structure is revealed to also contain a spiral structure. Spiral structures associated with circumstellar envelopes have been previously seen, leading to the conclusion that the systems must be binaries[5–8]. Combining the observational data with hydrodynamic simulations, we conclude that R Sculptoris is a binary system that underwent a thermal pulse about 1,800 years ago, lasting approximately 200 years. About 3×10^{-3} solar masses of material were ejected at a velocity of 14.3 km s^{-1} and at a rate around 30 times higher than the pre-pulse mass-loss rate. This shows that about three times more mass was returned to the interstellar medium during and immediately after the pulse than previously thought.

The detached shell around R Sculptoris was observed in CO($J = 3 - 2$) emission at 345 GHz using the Atacama Large Millimeter/submillimeter Array (ALMA) during Cycle 0 operations (Fig. 1 and Supplementary Information). The data clearly show the well-centred detached shell with a radius of 18.5″, and reveal a spiral structure extending from the central star outwards to the shell. Previous observations of R Sculptoris show structure in the form of clumps. However, this was interpreted as clumpy material within the shell itself, and not as a structure interior to the shell[2].

Until now no clear signs of binary companions have been observed in any detached shell sources (with a possible exception for the detached shell around TT Cygnus[9]). The observed structure around R Sculptoris, however, indicates the presence of a companion, shaping the stellar wind into a spiral shell structure[8]. Smoothed particle hydrodynamics (SPH) models show that a wide binary companion can have a significant effect in the shaping of the wind, leading to elliptical and spiral structures (for example, as observed in the case of the envelope of AFGL 3068)[5,6].

The observed shapes of the circumstellar envelopes around binary asymptotic-giant-branch stars depend on the physical parameters of the binary system (such as separation and mass ratio[10]), the density contrasts imprinted on the wind, the temperatures in the circumstellar envelope, the viewing angle, and the chemistry and excitation of the gas[11]. The temporal variations of the mass-loss rate and the expansion velocity further affect the structure of the circumstellar envelope. Hence, the observed spiral structure and detached shell allow us to measure these important properties, and to link them directly to the thermal pulse.

Any change in the expansion velocity of the stellar wind will affect the spacing between the spiral windings. In Fig. 2 the spiral can be followed from the central star out to the detached shell over about five windings. The 2.5 inner windings have a nearly constant spacing, with an average distance of 2.6″, implying an essentially constant expansion velocity during the last 2.5 orbital periods. The expansion velocity of the present-day wind[3] of R Sculptoris gives an orbital period of $t_{orb} = 350$ years. The position angle and radius of the observed emission then allow us to derive the velocity evolution of the stellar wind

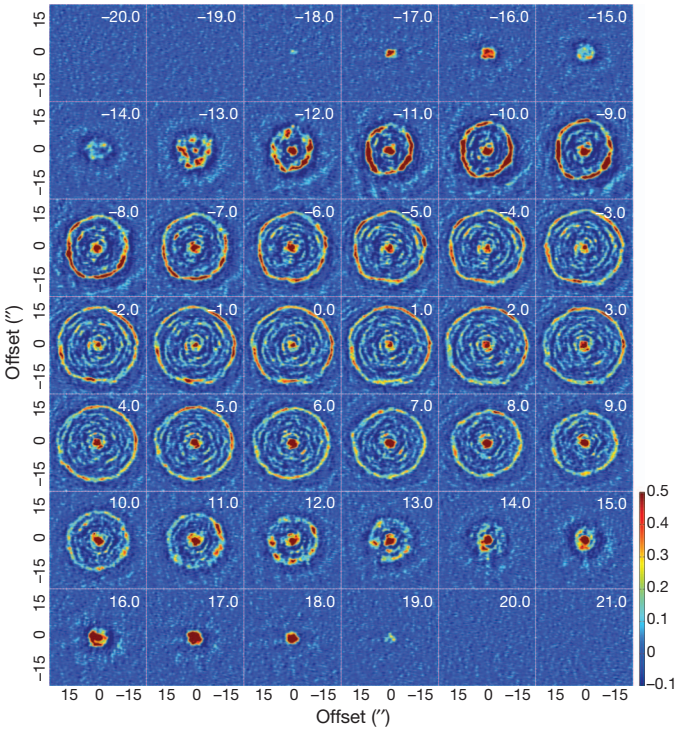

Figure 1 | ALMA Early Science observations of the CO($J = 3 - 2$) emission from the asymptotic-giant-branch star R Sculptoris. The figure shows the emission in the different velocity channels. The colour scale gives the flux in Jy per beam. The stellar velocity with respect to the local standard of rest (LSR) is $v_{LSR} = -19$ km s^{-1}. The numbers in the top right corners indicate the velocity in kilometres per second with respect to the stellar velocity. The spherical detached shell appears as a ring in the individual velocity channels, with its largest extent at the stellar velocity. The shell is clearly visible at 18.5″ at the stellar v_{LSR}, as well as a spiral structure connecting the central star with the detached shell. The structure can be traced through all velocity channels.

[1]European Southern Observatory, Karl-Schwarzschild-Strasse 2, 85748 Garching, Germany. [2]Argelander Institute for Astronomy, University of Bonn, Auf dem Hügel 71, 53121 Bonn, Germany. [3]South African Astronomical Observatory, PO Box 9, Observatory 7935, Cape Town, Western Cape, South Africa. [4]Onsala Space Observatory, Department of Earth and Space Sciences, Chalmers University of Technology, SE-43992 Onsala, Sweden. [5]Royal Observatory of Belgium, Ringlaan 3, 1180 Brussels, Belgium. [6]University of Vienna, Department of Astrophysics, Türkenschanzstrasse 17, 1180 Wien, Austria. [7]Joint ALMA Observatory, Alonso de Córdova 3107, Vitacura, Santiago, Chile.

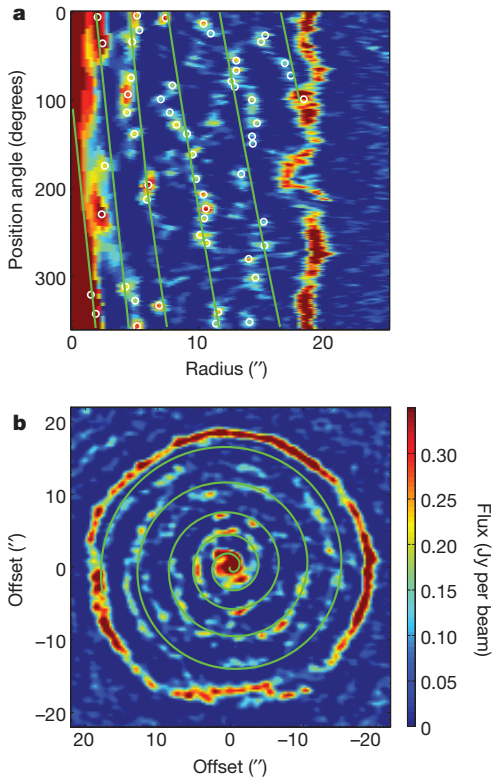

Figure 2 | The CO($J = 3 - 2$) emission at the stellar v_{LSR} of R Sculptoris. **a**, Position angle versus radius based on the stellar v_{LSR} image. The position angle starts at due North and increases counter-clockwise. **b**, The stellar v_{LSR} image. The colour scale gives the flux in Jy per beam. The green lines show linear fits to the emission peaks (white circles) in **a**. The first 2.5 windings are nearly parallel, with a constant separation of $2.6'' \pm 0.07''$, indicating that the expansion velocity has been constant (on average) for the last 2.5 binary periods. The present-day expansion velocity is estimated to be 10.5 km s^{-1}, giving a binary period of 350 years. The linear fits can hence be translated directly into a velocity evolution (Fig. 3). The corresponding spiral is plotted on top of the stellar v_{LSR} image (**b**). Deviations from a perfect spiral are of the order of ± 1.5 km s^{-1}, indicating small velocity variations over periods of 50 years. Partial spiral arms and arcs connecting the third and fourth windings show a larger variation in the wind velocity during these orbital periods on a timescale of about 100 years.

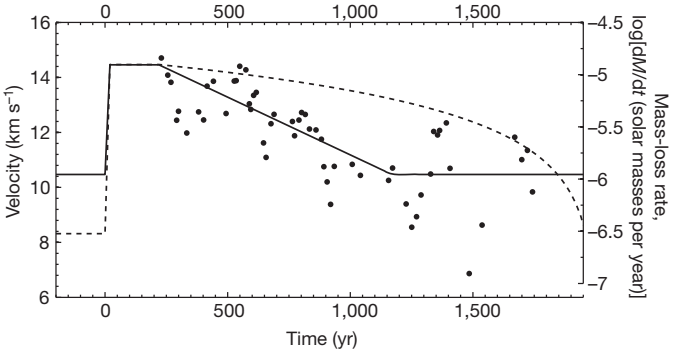

Figure 3 | The velocity and mass-loss rate evolution of the stellar wind around R Sculptoris. The solid and dashed lines show the velocity and mass-loss rate as a function of time, respectively. The points correspond to the expansion velocities of the emission peaks in Fig. 2a, assuming a binary period of 350 years. The figure shows the evolution of the velocity and mass-loss rate since the onset of the last thermal pulse. The velocity profile is a fit to the data points, whereas the mass-loss rate profile is constrained by the pre-pulse, pulse and present-day mass-loss rates. The profiles are used as input to the SPH models. The shape of the mass-loss rate profile is chosen to be consistent with the observations. The overall velocity fits the predictions from theoretical models of thermal pulses well. However, velocity variations of ± 1.5 km s^{-1} are apparent throughout the evolution since the last pulse, whereas theoretical models only predict significant variations in the expansion velocity less than 200 years after the pulse[4]. Theoretical models predict an increasing widening of the spiral proportional to the local sound speed, which may explain at least part of the velocity variation[8].

from R Sculptoris from the star out to the detached shell (Fig. 3, and Supplementary Information). The derived evolution of the expansion velocity since the last thermal pulse is consistent with models of thermal pulses[4]. However, the observed emission implies variations in the expansion velocity of ± 1.5 km s^{-1} on timescales of a few hundred years. Observed partial spiral windings and arcs, as well as emission at velocities up to 19 km s^{-1}, indicate brief periods of even larger velocity variations.

A spherically symmetric, detached shell can still be created in a binary system where the asymptotic-giant-branch star is undergoing a thermal pulse, owing to the brief increase in mass-loss rate and expansion velocity. Collision with the surrounding, slower material will then shape the wind into a symmetric shell structure. The post-pulse mass loss leaves behind a spiral structure that connects the detached shell with the central star. Assuming a spherically symmetric expanding detached shell gives a shell expansion velocity of $v_{sh} = 14.3$ km s^{-1} and a shell radius of $R_{sh} = 18.5''$ (see Supplementary Information).

The present expansion velocity and size of the shell around R Sculptoris put the upper limit to the end of the thermal pulse at 1,800 years ago. With a binary period of 350 years we would expect to see around five windings since the pulse, consistent with the observed spiral. A decelerated shell would imply a shorter time since the thermal pulse, and hence a shorter binary period or fewer spiral windings. The sweeping-up of material from the pre-pulse wind could cause such a deceleration of the shell. However, although a slight decrease in the expansion velocity of the detached shell is possible, we find no evidence of a noticeable decrease. This is contrary to the current theory of how detached shells are formed during thermal pulses[3,4]. Also, no material is likely to have piled onto the shell because of the post-pulse mass loss.

Recent images of thermal dust emission show the detached shell, as well as a more distant, and spatially distinct, region of interaction with the interstellar material[12], indicating the presence of a stellar wind from R Sculptoris before the pulse. Collision with a previous, slower wind is required to prevent the thin shell from quickly diffusing[4,13]. The average CO line intensity in the area surrounding the shell sets an upper limit to the pre-pulse mass-loss rate, and its ratio to the average CO line intensity in the shell suggests an increase in mass-loss rate during the thermal pulse by a factor of more than ten. The total shell mass is essentially only due to the mass lost during the formation of the shell. An estimated total gas mass in the shell of 2.5×10^{-3} solar masses (ref. 3) gives a thermal pulse mass-loss rate of between 7×10^{-6} solar masses per year and 2.5×10^{-5} solar masses per year (see Supplementary Information), and implies a pre-pulse mass-loss-rate of less than 10^{-6} solar masses per year. The present-day mass-loss rate is estimated to be 3×10^{-7} solar masses per year (ref. 3), that is, a factor of about 30 lower than during the pulse. This general evolution of the mass-loss rate is consistent with stellar evolution models; however, the ratio between the derived pulse and pre-pulse mass-loss-rate is significantly higher than found in the models[4].

To further constrain the mass-loss-rate evolution of R Sculptoris, we modelled the system with a modified version of the GADGET-2 SPH code[14], including detailed radiative cooling[15]. The modelled system successfully forms a detached shell, including the observed spiral structure (see Supplementary Video). The modelled density, temperature and velocity structures of the SPH model are then used as input in the three-dimensional radiative transfer code LIME[16]. The global morphology of the modelled system closely resembles that of the observations, and the brightness distribution reproduces the observed intensities well (Fig. 4). We effectively constrain the mass-loss-rate evolution

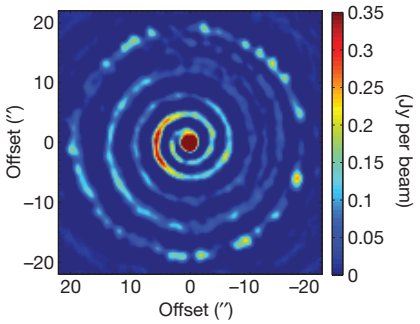

Figure 4 | LIME radiative transfer model of the circumstellar structure around R Sculptoris. The model is based on the results from the SPH models at the stellar velocity. The results of the radiative transfer model have been processed by the 'simdata' task in CASA (Common Astronomy Software Applications) using the ALMA Cycle 0 compact configuration specifications. The colour scale gives the flux in Jy per beam. The overall model intensities match the observed intensities well, while variations in the intensity contrast between the spiral windings and interwinding material indicate a more complicated mass-loss rate variation. The inclination angle of the binary system to the line of sight is 90°. See Supplementary Information for an animation of the SPH models of R Sculptoris.

throughout the thermal pulse to the present time (Fig. 3). Assuming an inter-pulse time of 50,000 years (typical for stars of about 1−4 solar masses; ref. 17) and our derived mass-loss rate evolution, 10% of the mass lost between two subsequent pulses is expelled during the thermal pulse, and 40% is lost during the first 1,800 years after the pulse. The pulse and immediate post-pulse phases are therefore dominant in the formation and chemical enrichment of the circumstellar envelope.

The chemical content of the expelled material depends critically on the physical properties of the pulses (for example, pulse duration and interpulse mass-loss rate). The duration of the pulse limits the time for nucleosynthesis to occur inside the star[18], whereas the mass-loss rate between pulses limits the number of thermal pulses an asymptotic-giant-branch star will experience[17]. These properties will affect the stellar yields of new elements returned to the interstellar medium, as well as eventually lead to the termination of the asymptotic-giant-branch phase. The observations presented here directly constrain these important physical parameters throughout the thermal-pulse cycle. In essence, it is the observed spiral structure that allows us to verify model results observationally, and refine our knowledge of thermal pulses and late stellar evolution.

Received 20 April; accepted 10 August 2012.

1. Olofsson, H., Eriksson, K. & Gustafsson, B. SEST CO (J = 1 - 0) observations of carbon-rich circumstellar envelopes. *Astron. Astrophys.* **196,** L1–L4 (1988).
2. Olofsson, H., Maercker, M., Eriksson, K., Gustafsson, B. & Schöier, F. High-resolution HST/ACS images of detached shells around carbon stars. *Astron. Astrophys.* **515,** A27 (2010).
3. Schöier, F. L., Lindqvist, M. & Olofsson, H. Properties of detached shells around carbon stars. Evidence of interacting winds. *Astron. Astrophys.* **436,** 633–646 (2005).
4. Mattsson, L., Höfner, S. & Herwig, F. Mass loss evolution and the formation of detached shells around TP-AGB stars. *Astron. Astrophys.* **470,** 339–352 (2007).
5. Mastrodemos, N. & Morris, M. Bipolar pre-planetary nebulae: hydrodynamics of dusty winds in binary systems. II. Morphology of the circumstellar envelopes. *Astrophys. J.* **523,** 357–380 (1999).
6. Mauron, N. & Huggins, P. J. Imaging the circumstellar envelopes of AGB stars. *Astron. Astrophys.* **452,** 257–268 (2006).
7. Dinh-V-Trung & Lim, J. Tracing the asymmetry in the envelope around the carbon star CIT 6. *Astrophys. J.* **701,** 292–297 (2009).
8. Kim, H. & Taam, R. E. Probing substellar companions of asymptotic giant branch stars through spirals and arcs. *Astrophys. J.* **744,** 136 (2012).
9. Olofsson, H. *et al.* A high-resolution study of episodic mass loss from the carbon star TT Cygni. *Astron. Astrophys.* **353,** 583–597 (2000).
10. De Marco, O. The origin and shaping of planetary nebulae: putting the binary hypothesis to the test. *Publ. Astron. Soc. Pacif.* **121,** 316–342 (2009).
11. Politano, M. & Taam, R. E. The incidence of non-spherical circumstellar envelopes in asymptotic giant branch stars. *Astrophys. J.* **741,** 5 (2011).
12. Cox, N. L. J. *et al.* A far-infrared survey of bowshocks and detached shells around AGB stars and red supergiants. *Astron. Astrophys.* **537,** A35 (2012).
13. Steffen, M. & Schönberner, D. On the origin of thin detached gas shells around AGB stars. Insights from time-dependent hydrodynamical simulations. *Astron. Astrophys.* **357,** 180–196 (2000).
14. Springel, V. The cosmological simulation code GADGET-2. *Mon. Not. R. Astron. Soc.* **364,** 1105–1134 (2005).
15. Mohamed, S. & Podsiadlowski, P. in *15th European Workshop on White Dwarfs* (eds R. Napiwotzki & M. R. Burleigh) 397–400 (Astronomical Society of the Pacific Conference Series 372, 2007).
16. Brinch, C. & Hogerheijde, M. R. LIME—a flexible, non-LTE line excitation and radiation transfer method for millimeter and far-infrared wavelengths. *Astron. Astrophys.* **523,** A25 (2010).
17. Karakas, A. & Lattanzio, J. C. Stellar models and yields of asymptotic giant branch stars. *Publ. Astron. Soc. Aust.* **24,** 103–117 (2007).
18. Busso, M., Gallino, R. & Wasserburg, G. J. Nucleosynthesis in asymptotic giant branch stars: relevance for galactic enrichment and solar system formation. *Annu. Rev. Astron. Astrophys.* **37,** 239–309 (1999).

Supplementary Information is available in the online version of the paper.

Acknowledgements This paper makes use of ALMA data from project no. ADS/JAO.ALMA#2011.0.00131.S. ALMA is a partnership of ESO (representing its member states), the NSF (USA) and NINS (Japan), together with the NRC (Canada) and NSC and ASIAA (Taiwan), in cooperation with the Republic of Chile. The Joint ALMA Observatory is operated by ESO, AUI/NRAO and NAOJ. We gratefully acknowledge the technical expertise and assistance provided by the Spanish Supercomputing Network (Red Espanola de Supercomputacion), as well as the use of the LaPalma Supercomputer, located at the Instituto de Astrofisica de Canarias. F.K. acknowledges funding by the Austrian Science Fund FWF under project numbers P23586-N16 and I163-N16. C.P. acknowledges funding by the Austrian Science Fund FWF under project number P23006-N16.

Author Contributions M.M. planned the project, prepared and submitted the proposal, analysed the data, and wrote the manuscript. S.M. was involved in project preparation, data interpretation, did the SPH modelling, and commented on the manuscript. W.V. was involved in project planning, proposal preparation, data reduction and analysis, radiative transfer modelling, and commented on the manuscript. S.R. was involved in project planning, data analysis, and commented on the manuscript. The remaining authors were involved in the project preparation, science discussion, and commented on the manuscript.

Author Information Reprints and permissions information is available at www.nature.com/reprints. The authors declare no competing financial interests. Readers are welcome to comment on the online version of the paper. Correspondence and requests for materials should be addressed to M.M. (mmaercke@eso.org).